

Verifying message-passing neural networks via topology-based bounds tightening

Christopher Hojny^{*1}, Shiqiang Zhang², Juan S. Campos², and Ruth Misener²

¹*Eindhoven University of Technology, Eindhoven, The Netherlands*
email *c.hojny@tue.nl*

²*Department of Computing, Imperial College London, UK*
email *{s.zhang21, juan.campos-salazar12, r.misener}@imperial.ac.uk*

February 22, 2024

Abstract

Since graph neural networks (GNNs) are often vulnerable to attack, we need to know when we can trust them. We develop a computationally effective approach towards providing robust certificates for message-passing neural networks (MPNNs) using a Rectified Linear Unit (ReLU) activation function. Because our work builds on mixed-integer optimization, it encodes a wide variety of subproblems, for example it admits (i) both adding and removing edges, (ii) both global and local budgets, and (iii) both topological perturbations and feature modifications. Our key technology, topology-based bounds tightening, uses graph structure to tighten bounds. We also experiment with aggressive bounds tightening to dynamically change the optimization constraints by tightening variable bounds. To demonstrate the effectiveness of these strategies, we implement an extension to the open-source branch-and-cut solver SCIP. We test on both node and graph classification problems and consider topological attacks that both add and remove edges.

1 Introduction

Graph neural networks (GNNs) may have incredible performance in graph-based tasks, but researchers also raise concerns about their vulnerability: small input changes sometimes lead to wrong GNN predictions (Günemann, 2022). To study these GNN vulnerabilities, prior works roughly divide into two classes: adversarial attacks (Dai et al., 2018; Zügner et al., 2018; Takahashi, 2019; Xu et al., 2019; Zügner & Günemann, 2019b; Chen et al., 2020; Ma et al., 2020; Sun et al., 2020; Wang et al., 2020; Geisler et al., 2021) and certifiable robustness (Bojchevski & Günemann, 2019; Zügner & Günemann, 2019a, 2020; Bojchevski et al., 2020; Jin et al., 2020; Sälzer & Lange, 2023). Beyond the difficulties of developing adversarial robustness for dense neural networks (Lomuscio & Maganti, 2017; Fischetti & Jo, 2018), incorporating graphs brings new challenges to both adversarial attacks and certifiable robustness. The first difficulty is defining graph perturbations because, beyond tuning the features (Takahashi, 2019; Zügner et al., 2018; Zügner & Günemann, 2019a; Bojchevski et al., 2020; Ma et al., 2020), an attacker may inject nodes (Sun et al., 2020; Wang et al., 2020) or add/delete edges (Dai et al., 2018; Zügner et al., 2018; Bojchevski & Günemann, 2019; Zügner & Günemann, 2019b, 2020; Xu et al., 2019; Chen et al., 2020; Jin et al., 2020; Geisler et al., 2021). Second, binary elements in the adjacency matrix create discrete optimization problems. Finally, perturbations to a node may indirectly attack other nodes via message passing or graph convolution.

^{*}Corresponding author

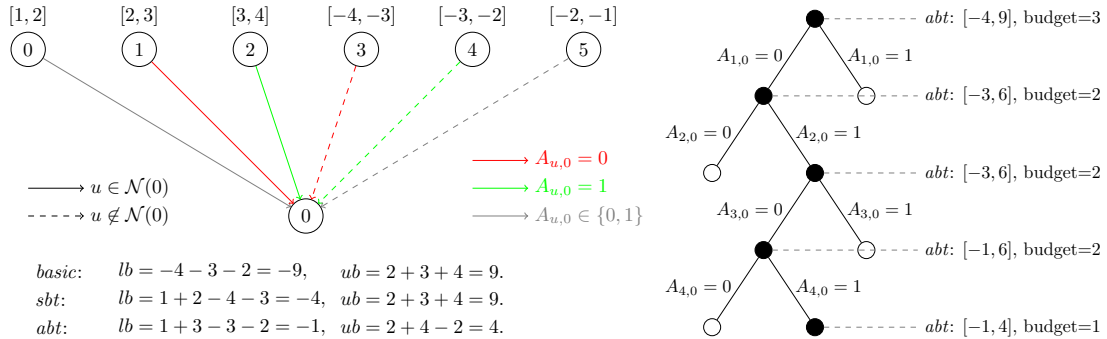


Figure 1: (left) Consider a graph with 6 nodes and a single feature. The input bounds are given above each node. Assume the budget for node 0 is 3, and 4 decisions have been made in the branch-and-bound tree, i.e., the binary variables representing the adjacency matrix are set as $A_{1,0} = 0, A_{2,0} = 1, A_{3,0} = 0, A_{4,0} = 1$. Since $\mathcal{N}(0) = \{0, 1, 2\}$ is the original neighbor set of node 0, fixing $A_{2,0} = 1$ and $A_{3,0} = 0$ spends no budget. For each method, we compute the bounds for node 0 in the next layer. To compute a lower bound, *basic* chooses all negative lower bounds without considering either budgets or previous decisions in the branch-and-bound tree. Static bounds tightening or *sbt*, the first topology-based bounds tightening routine, removes node 2 and adds node 3 and node 4 as neighbors within 3 budgets, but ignores previous decisions in the branch-and-bound tree. Aggressive bounds tightening or *abt* yields the tightest bounds by saving node 0 and adding node 5 as neighbors. (right) The branch-and-bound tree corresponding to the left. We provide the bounds yielded from *abt* and budget left after each decision.

Adversarial attacks aim to change the predictions of a GNN with admissible perturbations. In graph classification, the attacking goal is the prediction of a target graph (Dai et al., 2018; Chen et al., 2020). In node classification, attacks may be *local* (or targeted) and *global* (or untargeted). Local attacks (Dai et al., 2018; Zügner et al., 2018; Takahashi, 2019; Wang et al., 2020) try to change the prediction of a single node under perturbations, and global attacks (Xu et al., 2019; Zügner & Günnemann, 2019b; Ma et al., 2020; Sun et al., 2020; Geisler et al., 2021) allow perturbations to a group of nodes. Except for the Q-learning approach and genetic algorithm of Dai et al. (2018), most aforementioned works are first-order methods which derive or approximate gradients w.r.t. features and edges. Binary variables are flipped when they are chosen to be updated.

Certifiable robustness tries to guarantee that the prediction will not change under any admissible GNN perturbation. The state-of-the-art (Bojchevski & Günnemann, 2019; Zügner & Günnemann, 2019a, 2020; Bojchevski et al., 2020; Jin et al., 2020) typically formulates certifiable robustness as a constrained optimization problem, where the objective is the worst-case margin between the correct class and other class(es), and the constraints represent admissible perturbations (Günnemann, 2022). Given a GNN and a target node/graph, a certificate requires proving that the objective is always positive. Any feasible solution with a negative objective is an adversarial attack. Most existing certificates (Zügner & Günnemann, 2019a; Bojchevski et al., 2020; Jin et al., 2020) focus on graph convolutional networks (GCNs) (Kipf & Welling, 2017). The certificate on personalized propagation of neural predictions (Gasteiger et al., 2019) relies on local budget and yields looser guarantees in the presence of a global budget (Bojchevski & Günnemann, 2019). Also, each certificate has specific requirements on the perturbation type, e.g., changing node features only (Zügner & Günnemann, 2019a; Bojchevski et al., 2020), modifying graph structure only (Bojchevski & Günnemann, 2019; Jin et al., 2020), removing edges only (Zügner & Günnemann, 2020), and allowing only orthogonal Gromov-Wasserstein threats (Jin et al., 2022). Instead of verifying GNNs directly, Wang et al. (2021) use random smoothing (Cohen et al., 2019) to explore the robustness of smoothed GNN classifiers.

This work develops certificates on the classic message passing framework, especially GraphSAGE (Hamilton et al., 2017). Using a recently-proposed mixed-integer formulation for GNNs (McDonald et al., 2023; Zhang et al., 2023a,b), we directly encode a GNN into an optimization problem using linear constraints. Many perturbations are compatible with our formulation: (i) both adding and removing edges, (ii) both global and local budgets, and (iii) both topological perturbations and feature modifications.

When verifying fully-dense, feed-forward neural networks with ReLU activation, prior work shows that tightening variable bounds in a big-M formulation (Anderson et al., 2020) may lead to better

computational performance (Tjeng et al., 2019; Botoeva et al., 2020; Tsay et al., 2021; Badilla et al., 2023; Zhao et al., 2024). Since tighter variable bounds may improve the objective value of relaxations of the big-M formulation, they may be useful when providing a certificate of robustness. Because the optimization problems associated with verifying MPNNs are so large, this work cannot use any of the tighter, convex-hull based optimization formulations (Singh et al., 2019; Tjandraatmadja et al., 2020; Müller et al., 2022). Instead, we use what we call *topology-based bounds tightening* to enable a much stronger version of feasibility-based bounds tightening: we extend SCIP (Bestuzheva et al., 2023) to explicitly use the graph structures. We also develop an *aggressive bounds tightening* (Belotti et al., 2016) routine to dynamically change the optimization constraints by tightening variable bounds within SCIP. Key outcomes include: (i) solving literature node classification instances in a fraction of a second, (ii) solving an extra 266 graph classification instances after implementing topology-based bounds tightening in SCIP, and (iii) making the open-source solver SCIP nearly as performant as the commercial solver Gurobi, e.g., improving the time penalty of the open-source solver from a factor of 10 to a factor of 3 for robust instances.

The paper begins in Section 2 by defining a mixed-integer encoding for MPNNs. Section 3 presents the verification problem and develops our two topology-based bounds tightening routines, static bounds tightening *sbt* and aggressive bounds tightening *abt*. Section 4 presents the numerical experiments and Section 5 concludes. Figure 1 represents a toy example showing the basic approach in comparison to our two topology-based approaches *sbt* and *abt*.

2 Definition & Encoding of MPNNs

We inherit the mixed-integer formulation of MPNNs from Zhang et al. (2023a) and formulate ReLU activation using big-M (Anderson et al., 2020). Consider a trained GNN:

$$f : \mathbb{R}^{N \times d_0} \times \{0, 1\}^{N \times N} \rightarrow \mathbb{R}^{N \times d_L} \quad (1)$$

$$(X, A) \mapsto f(X, A)$$

whose l -th layer with weights $\mathbf{w}_{u \rightarrow v}^{(l)}$ and biases $\mathbf{b}_v^{(l)}$ is:

$$\mathbf{x}_v^{(l)} = \sigma \left(\sum_{u \in \mathcal{N}(v) \cup \{v\}} \mathbf{w}_{u \rightarrow v}^{(l)} \mathbf{x}_u^{(l-1)} + \mathbf{b}_v^{(l)} \right) \quad (2)$$

where $v \in V$, $V = \{0, 1, \dots, N-1\}$ is the node set, $\mathcal{N}(v)$ is the neighbor set of node v , and σ is activation. Given input features $\{\mathbf{x}_v^{(0)}\}_{v \in V}$ and the graph structure, we can derive the hidden features $\{\mathbf{x}_v^{(l)}\}_{v \in V}$, $\mathbf{x}_v^{(l)} \in \mathbb{R}^{d_l}$. When $l = L$, we obtain the node representation $\mathbf{x}_v^{(L)}$ of each node.

2.1 Big-M formulation for MPNNs

When the graph structure is not fixed, we need to include all possible contributions from all nodes, i.e., the l -th layer is:

$$\mathbf{x}_v^{(l)} = \sigma \left(\sum_{u \in V} A_{u,v} \mathbf{w}_{u \rightarrow v}^{(l)} \mathbf{x}_u^{(l-1)} + \mathbf{b}_v^{(l)} \right) \quad (3)$$

where $A_{u,v} \in \{0, 1\}$ controls the existence of edge $u \rightarrow v$.

With fixed weights and biases, we still need to handle the nonlinearities caused by (i) bilinear terms $A_{u,v} \mathbf{x}_u^{(l-1)}$, and (ii) activation σ . Let $\bar{\mathbf{x}}_v^{(l)} = \sum_{u \in V} A_{u,v} \mathbf{w}_{u \rightarrow v}^{(l)} \mathbf{x}_u^{(l-1)} + \mathbf{b}_v^{(l)}$, the Zhang et al. (2023b) big-M

formulation introduces auxiliary variables $\mathbf{x}_{u \rightarrow v}^{(l-1)}$ to replace the bilinear terms $A_{u,v} \mathbf{x}_u^{(l-1)}$ and linearly encodes $\bar{\mathbf{x}}_v^{(l)}$:

$$\bar{\mathbf{x}}_v^{(l)} = \sum_{u \in V} \mathbf{w}_{u \rightarrow v}^{(l)} \mathbf{x}_{u \rightarrow v}^{(l-1)} + \mathbf{b}_v^{(l)}. \quad (4)$$

Let $F_l := \{0, 1, \dots, d_l - 1\}$ and denote the f -th element of $\mathbf{x}_*^{(l)}$ by $x_{*,f}^{(l)}$, $f \in F_l$. Use $lb(\cdot)$ and $ub(\cdot)$ to represent the lower and upper bound of a variable, respectively. Then $x_{u \rightarrow v, f}^{(l-1)} = A_{u,v} x_{u,f}^{(l-1)}$ is equivalently formulated in the following big-M constraints:

$$x_{u \rightarrow v, f}^{(l-1)} \geq lb(x_{u,f}^{(l-1)}) \cdot A_{u,v} \quad (5a)$$

$$x_{u \rightarrow v, f}^{(l-1)} \leq ub(x_{u,f}^{(l-1)}) \cdot A_{u,v} \quad (5b)$$

$$x_{u \rightarrow v, f}^{(l-1)} \leq x_{u,f}^{(l-1)} - lb(x_{u,f}^{(l-1)}) \cdot (1 - A_{u,v}) \quad (5c)$$

$$x_{u \rightarrow v, f}^{(l-1)} \geq x_{u,f}^{(l-1)} - ub(x_{u,f}^{(l-1)}) \cdot (1 - A_{u,v}). \quad (5d)$$

2.2 Big-M formulation for ReLU

When using ReLU as the activation, i.e.,

$$x_{v,f}^{(l)} = \max\{0, \bar{x}_{v,f}^{(l)}\}, \quad (6)$$

Anderson et al. (2020) proposed a big-M formulation:

$$x_{v,f}^{(l)} \geq 0 \quad (7a)$$

$$x_{v,f}^{(l)} \geq \bar{x}_{v,f}^{(l)} \quad (7b)$$

$$x_{v,f}^{(l)} \leq \bar{x}_{v,f}^{(l)} - lb(\bar{x}_{v,f}^{(l)}) \cdot (1 - \sigma_{v,f}^{(l)}) \quad (7c)$$

$$x_{v,f}^{(l)} \leq ub(\bar{x}_{v,f}^{(l)}) \cdot \sigma_{v,f}^{(l)} \quad (7d)$$

where $\sigma_{v,f}^{(l)} \in \{0, 1\}$ controls the on/off of the activation:

$$x_{v,f}^{(l)} = \begin{cases} 0, & \sigma_{v,f}^{(l)} = 0 \\ \bar{x}_{v,f}^{(l)}, & \sigma_{v,f}^{(l)} = 1. \end{cases} \quad (8)$$

2.3 Bounds propagation

Eqs. (5) and (7) show the importance of variable bounds $lb(\cdot)$ and $ub(\cdot)$ or *big-M parameters*. Given the input feature bounds, we define bounds for auxiliary variables $x_{u \rightarrow v, f}^{(l-1)}$ and post-activation variables $x_{v,f}^{(l)}$. Using $x_{u \rightarrow v, f}^{(l-1)} = A_{u,v} x_{u,f}^{(l-1)}$, the bounds of $x_{u \rightarrow v, f}^{(l-1)}$ are:

$$lb(x_{u \rightarrow v, f}^{(l-1)}) = \min\{0, lb(x_{u,f}^{(l-1)})\} \quad (9a)$$

$$ub(x_{u \rightarrow v, f}^{(l-1)}) = \max\{0, ub(x_{u,f}^{(l-1)})\} \quad (9b)$$

with which we can use arithmetic propagation or feasibility-based bounds tightening to obtain bounds of $\bar{x}_{v,f}^{(l)}$ based on Eq. (4). Then, we use Eq. (6) to bound $x_{v,f}^{(l)}$:

$$lb(x_{v,f}^{(l)}) = \max\{0, lb(\bar{x}_{v,f}^{(l)})\} \quad (10a)$$

$$ub(x_{v,f}^{(l)}) = \max\{0, ub(\bar{x}_{v,f}^{(l)})\}. \quad (10b)$$

Without extra information, bounds defined in Eqs. (9) and (10) are the tightest possible. However, in a branch-and-bound tree, more and more variables will be fixed, which provides the opportunity to tighten the bounds. Additionally, in specific applications such as verification, the graph domain is restricted, allowing us to derive tighter bounds.

Remark 2.1. A MPNN with L message passing steps is suitable for node-level tasks. For graph-level tasks, there is usually a pooling layer after message passing to obtain a global representation and several dense layers thereafter as a final regressor/classifier. We omit these formulations since (i) linear pooling, e.g., mean and sum, is easily incorporated into our formulation, and (ii) dense layers are a special case of Eq. (2) with a single node.

3 Verification of MPNNs

3.1 Problem definition

First, consider node classification. Given a trained MPNN defined as Eq. (2), the number of classes is the number of output features, i.e., $\mathcal{C} = d_L$, and the predicted label of node t corresponds to the maximal logit, i.e., $c^* = \max_{c \in \mathcal{C}} f_{t,c}(X, A)$. Given an input (X^*, A^*) consisting of features X^* and adjacency matrix A^* , denote its predictive label for a target node t as c^* . The worst case margin between predictive label c^* and attack label c under perturbations $\mathcal{P}(\cdot)$ is:

$$m^t(c^*, c) := \min_{(X, A)} f_{t, c^*}(X, A) - f_{t, c}(X, A) \quad (11)$$

s.t. $X \in \mathcal{P}(X^*), A \in \mathcal{P}(A^*)$.

A positive $m^t(c^*, c)$ means that the logit of class c^* is always larger than class c . If $m^t(c^*, c) > 0$, for all $c \in \mathcal{C} \setminus \{c^*\}$, then any admissible perturbation can not change the label assigned to node t , that is, this MPNN is robust to node t .

For graph classification, instead of considering a single node, we want to know the worst case margin between two classes for a target graph, i.e.,

$$m(c^*, c) := \min_{(X, A)} f_{c^*}(X, A) - f_c(X, A) \quad (12)$$

s.t. $X \in \mathcal{P}(X^*), A \in \mathcal{P}(A^*)$.

In both problems, the target graph (X^*, A^*) and predictive label c^* are fixed. For node classification, the target node t is also given. Therefore, we omit t in Eq. (11) and reduce both problems to one as shown in Eq. (12).

3.2 Admissible perturbations

The perturbations on features and edges can be described similarly. Locally, we may only change features/edges for each node with a given local budget. Also, there is typically a global budget for the number of changes. The feature perturbations are typically easier to implement since they will not hurt the message passing scheme, i.e., the graph structure is fixed. In such settings, there is no need to use the mixed-integer formulations for MPNNs in Section 2.1 since a message passing step is actually simplified as a dense layer. Since feature perturbations are well-studied (Zügner & Günnemann, 2019a) and our proposed bounds tightening techniques mainly focus on changeable graph structures, our computational results only consider the perturbations on the adjacency matrix.

We first define the admissible perturbations for undirected graphs, which admits both adding and removing edges. Denote the global budget by Q and local budget to node v by q_v , then the

perturbations $\mathcal{P}_1(A^*)$ are defined as:

$$\begin{aligned} \mathcal{P}_1(A^*) = \{ & A \in \{0, 1\}^{N \times N} \mid A = A^T, \\ & \|A - A^*\|_0 \leq 2Q, \\ & \|A_v - A_v^*\|_0 \leq q_v, \forall v \in V \} \end{aligned} \quad (13)$$

where A_v is the v -th column of A . $\mathcal{P}_1(\cdot)$ will be used in graph classification since the graphs in benchmarks are usually undirected and relatively small.

For node classification, literature benchmarks usually (i) are large directed graphs, e.g., 3000 nodes, (ii) have many node features, e.g., 3000 features, (iii) have small average degree, e.g., $1 \sim 3$. If admitting adding edges, then the graph domain is too large to optimize over. Therefore, the state-of-the-art (Zügner & Günnemann, 2020) only considers removing edges, where a L -hop neighborhood around the target node t is sufficient. For a MPNN with L message passing steps without perturbations, nodes outside a L -hop neighborhood cannot affect the prediction of t . Since adding edges is not allowed, the L -hop neighborhood of t after perturbations is always a subset of the previous neighborhood. Similar to the literature, we define a more restrictive perturbation space for large graphs:

$$\begin{aligned} \mathcal{P}_2(A^*) = \{ & A \in \{0, 1\}^{N \times N} \mid \\ & A_{u,v} \leq A_{u,v}^*, \forall u, v \in V, \\ & \|A - A^*\|_0 \leq Q, \\ & \|A_v - A_v^*\|_0 \leq q_v, \forall v \in V \} \end{aligned} \quad (14)$$

where global budget is replaced by Q since the graph is directed. $\mathcal{P}_2(\cdot)$ will be used in node classification. For our later analysis, however, we focus on $\mathcal{P}_1(\cdot)$ since $\mathcal{P}_2(\cdot)$ is more like a special case without adding edges.

3.3 Static bounds tightening

Note that large budgets in Eq. (13) make the verification problems meaningless since the perturbed graph could be any graph. The very basic assumption is that the perturbed graph is similar to the original one, which brings us to propose the first bounds tightening approach. The rough idea is to consider budgets when computing bounds of $\bar{x}_v^{(l)}$ based on bounds of $x_{u \rightarrow v}^{(l-1)}$ in Eq. (4). Instead of considering all contributions from all nodes, we first calculate the bounds based on original neighbors and then maximally perturb the bounds with given budgets. Mathematically, $lb(\bar{x}_{v,f'}^{(l)})$ is found by solving the following optimization problem:

$$\begin{aligned} \min_{A, x_{u,f}^{(l-1)}} \quad & \sum_{u \in V} A_{u,v} \sum_{f \in F_{l-1}} w_{u \rightarrow v, f \rightarrow f'}^{(l)} x_{u,f}^{(l-1)} + b_{v,f'}^{(l)} \\ \text{s.t.} \quad & A \in \mathcal{P}_1(A^*) \end{aligned} \quad (15)$$

where $w_{u \rightarrow v, f \rightarrow f'}^{(l)}$ is the (f, f') -th element in $w_{u \rightarrow v}^{(l)}$.

Remark 3.1. For brevity, we omit the superscripts of layers for all variables, and subscripts of edges in weights, i.e., rewriting Eq. (15) as:

$$\begin{aligned} lb(\bar{x}_{v,f'}) = \min_{A, x_{u,f}^{(l-1)}} \quad & \sum_{u \in V} A_{u,v} \sum_{f \in F_{l-1}} w_{f,f'} x_{u,f} + b_{v,f'} \\ \text{s.t.} \quad & A \in \mathcal{P}_1(A^*). \end{aligned} \quad (16)$$

Property 3.2. *The optimal solution of Eq. (16) is given by:*

$$lb(\bar{x}_{v,f'}) = \sum_{u \in \mathcal{N}^*(v)} lb_{u \rightarrow v} + b_{v,f'} + \min_{|V_{ib}| \leq q_v} \sum_{u \in V_{ib}} \Delta_{u \rightarrow v} \quad (17)$$

where $\mathcal{N}^*(v)$ denotes the original neighbor set of node v , $lb_{u \rightarrow v}$ represents the contribution of node u to the lower bound of node v when u is a neighbor of v , $\Delta_{u \rightarrow v}$ denotes the change of lower bound of node v caused by modifying edge $u \rightarrow v$, V_{lb} is the set of nodes consisting of removed/added neighbors.

Calculating $lb_{u \rightarrow v}$ is straightforward:

$$lb_{u \rightarrow v} = \sum_{f \in F_{l-1}} w_{f,f'} \cdot \mathbb{I}_{w_{f,f'} \geq 0} \cdot lb(x_{u,f}) + \sum_{f \in F_{l-1}} w_{f,f'} \cdot \mathbb{I}_{w_{f,f'} < 0} \cdot ub(x_{u,f}) \quad (18)$$

which is used to derive $\Delta_{u \rightarrow v}$ as:

$$\Delta_{u \rightarrow v} = \begin{cases} -lb_{u \rightarrow v}, & u \in \mathcal{N}^*(v) \\ lb_{u \rightarrow v}, & u \notin \mathcal{N}^*(v) \end{cases} \quad (19)$$

where two cases correspond to removing neighbor u and adding u as a neighbor, respectively. Furthermore, the last minimal term in Eq. (17) equivalently means that choosing at most q_v smallest negative terms among $\{\Delta_{u \rightarrow v}\}_{u \in V}$. The time complexity to compute lower bounds following Eq. (17) for each feature in l -th layer is $O(N^2 d_{l-1} d_l + N \log N)$. Upper bounds could be defined similarly, which are not included here due to space limitation.

Remark 3.3. The plain strategy without considering graph structure and budgets *basic* is:

$$lb(\bar{x}_{v,f'}) = \sum_{u \in V} \min\{0, lb_{u \rightarrow v}\} \quad (20)$$

and the time complexity is $O(N^2 d_{l-1} d_l)$.

As shown in the example presented in the Figure 1 example, the bounds derived from *basic* is $[-9, 9]$, which is improved to $[-4, 9]$ after applying static bounds tightening *sbt*.

3.4 Aggressive bounds tightening

Consider any node in a branch-and-bound tree, values of several $A_{u,v}$ are already decided during the path from root to current node, with which we can further tighten bounds in the subtree rooted by this node. Belotti et al. (2016) refer to the idea of tightening bounds in the branch-and-bound tree as *aggressive bounds tightening*. In MPNN verification, there are three types of $A_{u,v}$ in Eq. (16): (i) $A_{u,v}$ is fixed to 0, (ii) $A_{u,v}$ is fixed to 1, and (iii) $A_{u,v}$ is not fixed yet. Denote $V_0 = \{u \in V \mid A_{u,v} = 0\}$ and $V_1 = \{u \in V \mid A_{u,v} = 1\}$, then Eq. (16) in the current node is restricted as:

$$lb(\bar{x}_{v,f'}) = \min_A \sum_{u \in V} A_{u,v} lb_{u \rightarrow v} + b_{v,f'} \quad (21)$$

s.t. $A \in \mathcal{P}_1(A^*)$
 $A_{u,v} = 0, \forall u \in V_0$
 $A_{u,v} = 1, \forall u \in V_1.$

Property 3.4. The optimal solution of Eq. (21) is given by:

$$lb(\bar{x}_{v,f'}) = \sum_{u \in (\mathcal{N}^*(v) \setminus V_0) \cup V_1} lb_{u \rightarrow v} + b_{v,f'} + \min_{V_{lb} \subseteq V \setminus (V_0 \cup V_1), |V_{lb}| \leq q'_v} \Delta_{u \rightarrow v} \quad (22)$$

where q'_v is the currently available budget for node v .

In Eq. (22), the first term sums over $(\mathcal{N}^*(v) \setminus V_0) \cup V_1$ to represent the contributions from current neighbors. The last term excludes all fixed edges and only considers changeable neighbors. Similarly, this minimal term equals to choose at most q'_v smallest negative terms among $\{\Delta_{u \rightarrow v}\}_{u \in V \setminus (V_0 \cup V_1)}$. q'_v is derived from the remaining local and global budgets:

$$q'_v = \min\{q_v - e_r(v) - e_a(v), 2Q - \sum_{u \in V} e_r(u) - \sum_{u \in V} e_a(u)\} \quad (23)$$

where $e_r(v) := |\mathcal{N}^*(v) \cap V_0|$ is the number of removed edges around node v , $e_a(v) := |V_1 \setminus \mathcal{N}^*(v)|$ is the number of added edges around node v .

Remark 3.5. The bounds tightening inside the branch-and-bound tree can be interpreted as applying the Section 3.3 bounds tightening to a modified target graph with a reduced budget. The spent budget changes the neighbors of node v from $\mathcal{N}^*(v)$ to $(\mathcal{N}^*(v) \setminus V_0) \cup V_1$.

As shown in Figure 1, aggressive bounds tightening *abt* gives tighter bounds $[-1, 4]$ comparing to *basic* and *sbt*. The branch-and-bound tree in Figure 1 shows *abt* in action.

Table 1: Information on benchmarks. For multiple graphs, we compute the average number of nodes and edges.

benchmark	#graphs	#nodes	#edges	#features	#classes
MUTAG	188	17.9	39.6	7	2
ENZYMES	600	32.6	124.3	3	6
Cora	1	2708	5429	1433	7
CiteSeer	1	3312	4715	3703	6

4 Experiments

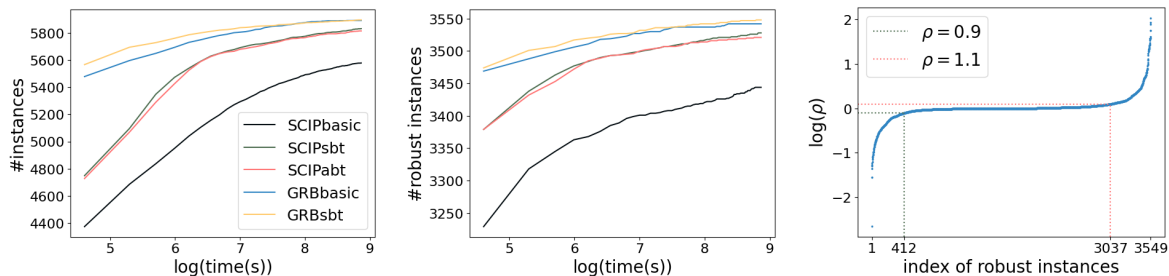


Figure 2: ENZYMES benchmark. (left) Number of instances solved by each method below different time costs. (middle) Number of robust instances solved by each method below different time costs. (right) Consider ρ , the ratio of time cost between SCIPabt and SCIPsbt on each robust instance. SCIPabt is at least 10% faster than SCIPsbt on 412 robust instances.

This section empirically evaluates the impact of static and aggressive bounds tightening on verifying MPNNs by solving a mixed-integer program (MIP) as shown in Section 2 and Section 3. All GNNs are built and trained using PyG (PyTorch Geometric) 2.1.0 (Fey & Lenssen, 2019). All MIPs are implemented in C/C++ using the open-source MIP solver SCIP 8.0.4 (Bestuzheva et al., 2023); all LP relaxations are solved using Soplex 6.0.4 (Gamrath et al., 2020). We used the GNN pull request (Zhang et al., 2023a) in the Optimization and Machine Learning Toolkit OMLT (Ceccon et al., 2022) to debug the implementation. Observe that we could have alternatively extended a similar tool in SCIP (Turner et al., 2023). For each verification problem, we apply the basic implementation (SCIPbasic), static bounds tightening (SCIPabt), and aggressive bounds tightening (SCIPsbt). Our experiments also

Table 2: Summary of results for graph classification. The approaches tested are SCIP basic (SCIPbasic), SCIP static bounds tightening (SCIPsbt), SCIP aggressive bounds tightening (SCIPabt), Gurobi basic (GRBbasic), and Gurobi static bounds tightening (GRBsbt). For each global budget, the number of instances is 600 for ENZYMES and 188 for MUTAG, but we only present comparisons when all methods give consistent results except for time out, as shown in column “#”. We compare times with respect to both average (“avg-time”) and the shifted geometric mean (“sgm-time”), as well as the number of solved instances within time limits 2 hours (“# solved”). Since robust instances are the ones where mixed-integer performance is most important (non-robust instances may frequently be found by more heuristic approaches), we also compare on the set of robust instances.

benchmark	method	all instances				robust instances			
		#	avg-time(s)	sgm-time(s)	# solved	#	avg-time(s)	sgm-time(s)	# solved
ENZYMES	SCIPbasic	5915	605.97	37.81	5579	3549	278.58	12.51	3444
	SCIPsbt	5915	230.59	21.26	5831	3549	82.89	6.65	3528
	SCIPabt	5915	246.02	21.77	5817	3549	88.95	6.71	3522
	GRBbasic	5915	86.03	7.59	5892	3549	32.80	2.82	3542
	GRBsbt	5915	74.87	7.09	5895	3549	22.90	2.50	3548
	MUTAG	SCIPbasic	1589	679.86	189.75	1575	44	798.47	202.93
MUTAG	SCIPsbt	1589	196.07	75.17	1589	44	336.41	100.86	44
	SCIPabt	1589	207.50	82.43	1589	44	238.10	91.11	44
	GRBbasic	1589	34.58	4.06	1589	44	162.25	12.11	44
	GRBsbt	1589	59.93	22.40	1589	44	73.78	15.00	44

include a basic and static bounds tightening implementation of Gurobi 10.0.3 (GRBbasic, GRBsbt) (Gurobi Optimization, LLC, 2023). The code is available by request and will be released open-source after peer review.

4.1 Implementation details

Our code models and solves the verification problem in three stages (for basic and static bounds tightening) or four stages (for aggressive bounds tightening). First, parameters of a trained MPNN (weights, biases) and the verification problem (predictive label c^* , attack label c , global budget Q , local budget q_v) are read. Second, lower and upper bounds on the variables in Eqs. (5) and (7) are computed for SCIPbasic and SCIPsbt. Third, a MIP model of the verification problem is created and solved. We do not solve the MIP models to global optimality as we only ask: *Is this instance robust or not?* We instead interrupt the optimization once a solution with negative objective value is found, i.e., the instance is non-robust, or the dual bound of the branch-and-bound tree is positive, i.e., the instance is robust.

In case of SCIPabt, the model is created as for static bounds tightening. During the solving process, a fourth step takes place. This step collects, at each node of the SCIP branch-and-bound tree, the A -variables that have been fixed to 0 and 1. We then iterate through the layers of the MPNN and, for each layer, we: (i) recompute the variable bounds as in the second step for the current layer, taking the fixed variables into account following Section 3.4; (ii) check if any inequality in Eqs. (5) and (7) using the newly computed bounds is violated by the current linear programming solution; (iii) if a violated inequality is detected, we add this inequality as a local cutting plane to the model. That is, we inform SCIP that the inequality is only valid at the current node of the branch-and-bound tree and all its children, which is necessary as the inequality is based on fixed variables at the current node. The separation of local cutting planes has been implemented via a separator callback in SCIP.

Besides our implementation in SCIP, we also conducted experiments using Gurobi 10.0.3 (Gurobi Optimization, LLC, 2023) to compare baseline (GRBbasic) and static bounds tightening (GRBsbt). We used our SCIP implementation to create the MIP models, store them on the hard drive, and read them via Gurobi’s Python interface. We did not investigate aggressive bounds tightening in Gurobi as Gurobi does not support local cutting planes. As for SCIP, we interrupt the solving process after deriving (non-) robustness.

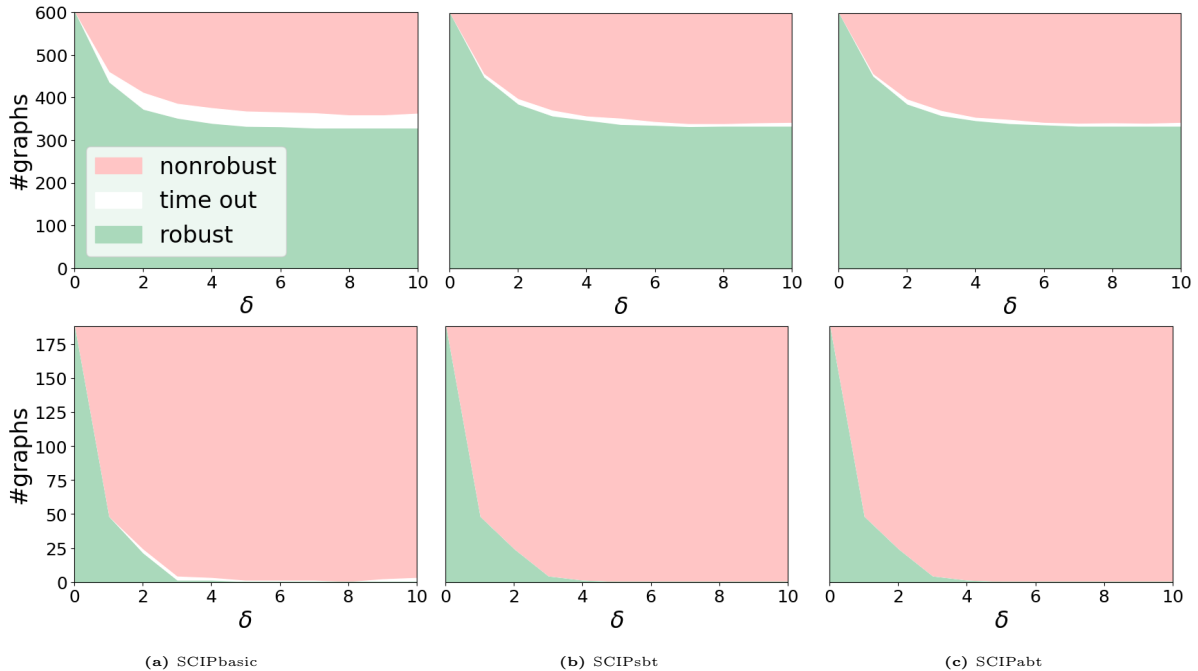


Figure 3: For each SCIP-based method on ENZYMES (the first row) and MUTAG (the second row), we count the number of robust graphs (green), nonrobust graphs (red), and time out (white). We exclude Gurobi-based methods in this figure since Gurobi conducts inconsistent results on some graphs.

4.2 Experimental setup

All experiments have been conducted on a Linux cluster with 12 Intel Xeon Platinum 8260 2.40 GHz processors each having 48 physical threads. Every model has been solved (either by SCIP or Gurobi) using a single thread. Due to the architecture of the cluster, the jobs have not been run exclusively. The reported running time in the following only consists of the time solving a model, but not creating it. That is, the time for computing the initial variable bounds for baseline and static bounds tightening are not considered, whereas the time for computing bounds in aggressive bounds tightening is considered since this takes place dynamically during the solving process.

We evaluate the performance of various verification methods on benchmarks including: (i) MUTAG and ENZYMES (Morris et al., 2020) for graph classification, and (ii) Cora and CiteSeer (Yang et al., 2023) for node classification. All datasets are available in PyG and summarized in Table 1. The attack label for each graph/node is fixed as $c = (c^* + 1) \bmod C$.

For graph classification, we train a MPNN with $L = 3$ SAGEConv (Hamilton et al., 2017) layers with 16 hidden channels, followed by an add pooling and a dense layer as the final classifier. Following Jin et al. (2020), 30% graphs are used to train the model. The local budget of each node is $q_v = \max\{0, d_v - \max_{u \in V} d_u + s\}$, where d_v is the degree of node v , s is the so-called local attack strength. In our experiments, we set $s = 2$, and use δ percentage of the number of edges as the global budget Q , where $1 \leq \delta \leq 10$.

For node classification, we train a MPNN with $L = 2$ SAGEConv layers with 32 hidden channels. Similar to Zügner & Günnemann (2020), 10% node labels are used for training. We set 10 as the global budget and 5 as the local budget. For each node, we extract its 2-hop neighborhood to build the corresponding verification problem. It is noteworthy that 2-hop neighborhood is sufficient for 2 message passing steps in MPNN, but insufficient for 2 graph convolutional steps in GCN. The reason is that removing an edge within a 3-hop neighborhood may influence the degree of a node within a 2-hop neighborhood.

All models are trained 200 epochs with learning rate 0.01, weight decay 10^{-4} , and dropout 0.5. We

set 2 hours as the time limit for verifying a graph in graph classification, and 30 minutes for verifying a node in node classification.

4.3 Numerical results

For each verification problem, we will get one of three results: robust (objective has non-negative lower bound), nonrobust (a feasible attack, i.e., solution with negative objective, is found), or time out (inconclusive within time limit). For each benchmark, we consider three criteria for each method: (i) average solving time (avg-time), (ii) shifted geometric mean (sgm-time) of solving time, and (iii) number of solved instances within time limit. A commonly used measure to compare MIP-based methods, the shifted geometric mean of t_1, \dots, t_n is $(\prod_{i=1}^n (t_i + s))^{1/n} - s$, where shift $s = 10$. Without the ground truth of each instance, we classify an instance as robust if all methods claim it is robust except for time out. Three criteria are evaluated for each method on each benchmark over all instances and all robust instances, respectively. We exclude all instances with inconsistencies, i.e., SCIP and Gurobi declares differently, for a fair comparison. See the appendix for more details.

For graph classification, we summarize the results for all instances in Table 2 and put full results in the appendix. Figure 2 visualizes the number of solved (robust) instances below different time costs, and compares the time costs between SCIPabt and SCIPsbt for ENZYMES. See the appendix for similar plots for MUTAG. Figure 3 plots the number of different types of graphs (robust, nonrobust, time out) with various global budgets for ENZYMES and MUTAG. The results for node classification are reported in Table 3 in the appendix. Only removing edges results in simple verification problems: all methods can solve all instances instantly. Adding more cutting planes is not helpful as this could hinder heuristics to find a feasible attack (in case of non-robustness) or result in solving more (difficult) LPs due to additional cutting planes (in case of robustness). Therefore, we skip the comparison with GRBbasic and GRBsbt.

As shown in Table 2, SCIPsbt is around three times faster than SCIPbasic and solves more instances within the same time limit. From the comparison between GRBbasic and GRBsbt, we can still notice the speed-up from static bounds tightening. Considering all instances from MUTAG, it seems like static bounds tightening slows down the solving process. The reason is that most MUTAG instances are not robust, i.e., finding good bounds on the objective value is unnecessary, finding a feasible attack instead is sufficient. Since bounds tightening mainly improves bounds on the objective, the complexity it add compared to the baseline thus may increase the time to find a feasible attack.

Our numerical results reflect similar performance between SCIPsbt and SCIPabt w.r.t. times in Table 2. SCIPabt might even be slower than SCIPsbt in some instances. This is because of the trade-off between the complexity of verification problem and budgets: More budget creates more complicated optimization problems, where we may benefit from aggressive bounds tightening. However, with enough budget, the instance is no longer robust. Then adding many cutting planes may slow down finding a feasible attack.

But, observe in Figure 2 that, of the 3549 robust instances from the ENZYMES benchmark, 412 are significantly faster when using SCIPabt and 512 are significantly faster when using SCIPsbt. Similarly for the MUTAG benchmark, 19 of the 44 robust instances are substantially faster using SCIPabt rather than SCIPsbt (see Figure 4). This is also reflected in Table 2 when considering the robust instances only. For the MUTAG instances (which are harder to solve than ENZYMES), SCIPabt is roughly 10% faster than SCIPsbt in shifted geometric mean (29% in arithmetic mean). This effect is even more pronounced for the most difficult MUTAG instances with a global budget of 2% and 3%, where SCIPabt is 10.8% and 22.0%, respectively, faster than SCIPsbt in shifted geometric mean (29.4% and 35.8% in arithmetic mean), see Table 5 in the appendix.

We therefore propose running SCIPsbt and SCIPabt in parallel, this idea corresponds to the common observation in MIP that parallelizing multiple strategies (here: SCIPsbt and SCIPabt) yields more benefits than parallelizing just one algorithm (Carvajal et al., 2014).

5 Conclusion

We propose topology-based bounds tightening approaches to verify message-passing neural networks. By exploiting graph structures and available budgets, our techniques compute tighter bounds for variables and thereby help certify robustness. Numerical results show the improvement of topology-based bounds tightening w.r.t. the solving time and the number of solved instances.

Acknowledgments

This work was supported by the Engineering and Physical Sciences Research Council [grant number EP/W003317/1], an Imperial College Hans Rausing PhD Scholarship to SZ, and a BASF/RAEng Research Chair in Data-Driven Optimisation to RM.

References

- Anderson, R., Huchette, J., Ma, W., Tjandraatmadja, C., and Vielma, J. P. Strong mixed-integer programming formulations for trained neural networks. *Mathematical Programming*, 183(1-2):3–39, 2020.
- Badilla, F., Goycoolea, M., Muñoz, G., and Serra, T. Computational tradeoffs of optimization-based bound tightening in relu networks, 2023.
- Belotti, P., Bonami, P., Fischetti, M., Lodi, A., Monaci, M., Nogales-Gómez, A., and Salvagnin, D. On handling indicator constraints in mixed integer programming. *Computational Optimization and Applications*, 65:545–566, 2016.
- Bestuzheva, K., Besançon, M., Chen, W.-K., Chmiela, A., Donkiewicz, T., van Doornmalen, J., Eifler, L., Gaul, O., Gamrath, G., Gleixner, A., et al. Enabling research through the SCIP optimization suite 8.0. *ACM Transactions on Mathematical Software*, 49(2):1–21, 2023.
- Bojchevski, A. and Günnemann, S. Certifiable robustness to graph perturbations. *NeurIPS*, 2019.
- Bojchevski, A., Gasteiger, J., and Günnemann, S. Efficient robustness certificates for discrete data: Sparsity-aware randomized smoothing for graphs, images and more. In *ICML*, 2020.
- Botoeva, E., Kouvaros, P., Kronqvist, J., Lomuscio, A., and Misener, R. Efficient verification of ReLU-based neural networks via dependency analysis. In *AAAI*, 2020.
- Carvajal, R., Ahmed, S., Nemhauser, G., Furman, K., Goel, V., and Shao, Y. Using diversification, communication and parallelism to solve mixed-integer linear programs. *Operations Research Letters*, 42(2):186–189, 2014.
- Ceccon, F., Jalving, J., Haddad, J., Thebelt, A., Tsay, C., Laird, C. D., and Misener, R. OMLT: Optimization & machine learning toolkit. *Journal of Machine Learning Research*, 23(349):1–8, 2022.
- Chen, J., Xu, H., Wang, J., Xuan, Q., and Zhang, X. Adversarial detection on graph structured data. In *PPMLP*, 2020.
- Cohen, J., Rosenfeld, E., and Kolter, Z. Certified adversarial robustness via randomized smoothing. In *ICML*, 2019.
- Dai, H., Li, H., Tian, T., Huang, X., Wang, L., Zhu, J., and Song, L. Adversarial attack on graph structured data. In *ICML*, 2018.
- Fey, M. and Lenssen, J. E. Fast graph representation learning with PyTorch Geometric. In *ICLR 2019 Workshop on Representation Learning on Graphs and Manifolds*, 2019.

- Fischetti, M. and Jo, J. Deep neural networks and mixed integer linear optimization. *Constraints*, 23(3):296–309, 2018.
- Gamrath, G., Anderson, D., Bestuzheva, K., Chen, W.-K., Eifler, L., Gasse, M., Gemander, P., Gleixner, A., Gottwald, L., Halbig, K., et al. The SCIP optimization suite 7.0. Technical Report 20-10, ZIB, Takustr. 7, 14195 Berlin, 2020.
- Gasteiger, J., Bojchevski, A., and Günnemann, S. Predict then propagate: Graph neural networks meet personalized pagerank. In *ICLR*, 2019.
- Geisler, S., Schmidt, T., Şirin, H., Zügner, D., Bojchevski, A., and Günnemann, S. Robustness of graph neural networks at scale. *NeurIPS*, 2021.
- Günnemann, S. Graph neural networks: Adversarial robustness. *Graph Neural Networks: Foundations, Frontiers, and Applications*, pp. 149–176, 2022.
- Gurobi Optimization, LLC. Gurobi Optimizer Reference Manual, 2023. URL <https://www.gurobi.com>.
- Hamilton, W., Ying, Z., and Leskovec, J. Inductive representation learning on large graphs. In *NeurIPS*, 2017.
- Jin, H., Shi, Z., Peruri, V. J. S. A., and Zhang, X. Certified robustness of graph convolution networks for graph classification under topological attacks. *NeurIPS*, 2020.
- Jin, H., Yu, Z., and Zhang, X. Certifying robust graph classification under orthogonal Gromov-Wasserstein threats. *NeurIPS*, 2022.
- Kipf, T. N. and Welling, M. Semi-supervised classification with graph convolutional networks. In *ICLR*, 2017.
- Lomuscio, A. and Maganti, L. An approach to reachability analysis for feed-forward ReLU neural networks. *arXiv preprint arXiv:1706.07351*, 2017.
- Ma, J., Ding, S., and Mei, Q. Towards more practical adversarial attacks on graph neural networks. *NeurIPS*, 2020.
- McDonald, T., Tsay, C., Schweidtmann, A. M., and Yorke-Smith, N. Mixed-integer optimisation of graph neural networks for computer-aided molecular design. *arXiv preprint arXiv:2312.01228*, 2023.
- Morris, C., Kriege, N. M., Bause, F., Kersting, K., Mutzel, P., and Neumann, M. TUDataset: A collection of benchmark datasets for learning with graphs. In *ICML 2020 Workshop on Graph Representation Learning and Beyond (GRL+ 2020)*, 2020.
- Müller, M. N., Makarchuk, G., Singh, G., Püschel, M., and Vechev, M. PRIMA: general and precise neural network certification via scalable convex hull approximations. *Proceedings of the ACM on Programming Languages*, 6(POPL):1–33, 2022.
- Sälzer, M. and Lange, M. Fundamental limits in formal verification of message-passing neural networks. In *ICLR*, 2023.
- Singh, G., Ganvir, R., Püschel, M., and Vechev, M. Beyond the single neuron convex barrier for neural network certification. In *NeurIPS*, pp. 15098–15109, 2019.
- Sun, Y., Wang, S., Tang, X., Hsieh, T.-Y., and Honavar, V. Adversarial attacks on graph neural networks via node injections: A hierarchical reinforcement learning approach. In *WWW*, 2020.
- Takahashi, T. Indirect adversarial attacks via poisoning neighbors for graph convolutional networks. In *IEEE Big Data*, 2019.

- Tjandraatmadja, C., Anderson, R., Huchette, J., Ma, W., PATEL, K. K., and Vielma, J. P. The convex relaxation barrier, revisited: Tightened single-neuron relaxations for neural network verification. In *NeurIPS*, volume 33, pp. 21675–21686, 2020.
- Tjeng, V., Xiao, K. Y., and Tedrake, R. Evaluating robustness of neural networks with mixed integer programming. In *ICLR*, 2019.
- Tsay, C., Kronqvist, J., Thebelt, A., and Misener, R. Partition-based formulations for mixed-integer optimization of trained ReLU neural networks. In *NeurIPS*, 2021.
- Turner, M., Chmiela, A., Koch, T., and Winkler, M. PySCIPOpt-ML: Embedding trained machine learning models into mixed-integer programs. *arXiv preprint arXiv:2312.08074*, 2023.
- Wang, B., Jia, J., Cao, X., and Gong, N. Z. Certified robustness of graph neural networks against adversarial structural perturbation. In *SIGKDD*, 2021.
- Wang, J., Luo, M., Suya, F., Li, J., Yang, Z., and Zheng, Q. Scalable attack on graph data by injecting vicious nodes. *Data Mining and Knowledge Discovery*, 34:1363–1389, 2020.
- Xu, K., Chen, H., Liu, S., Chen, P.-Y., Weng, T.-W., Hong, M., and Lin, X. Topology attack and defense for graph neural networks: An optimization perspective. *IJCAI*, 2019.
- Yang, R., Shi, J., Xiao, X., Yang, Y., Bhowmick, S. S., and Liu, J. PANE: scalable and effective attributed network embedding. *The VLDB Journal*, pp. 1–26, 2023.
- Zhang, S., Campos, J. S., Feldmann, C., Sandfort, F., Mathea, M., and Misener, R. Augmenting optimization-based molecular design with graph neural networks. *arXiv preprint arXiv:2312.03613*, 2023a.
- Zhang, S., Campos, J. S., Feldmann, C., Walz, D., Sandfort, F., Mathea, M., Tsay, C., and Misener, R. Optimizing over trained GNNs via symmetry breaking. In *NeurIPS*, 2023b.
- Zhao, H., Hijazi, H., Jones, H., Moore, J., Tanneau, M., and Van Hentenryck, P. Bound tightening using rolling-horizon decomposition for neural network verification. *arXiv preprint arXiv:2401.05280*, 2024.
- Zügner, D. and Günnemann, S. Certifiable robustness and robust training for graph convolutional networks. In *SIGKDD*, 2019a.
- Zügner, D. and Günnemann, S. Adversarial attacks on graph neural networks via meta learning. In *ICLR*, 2019b.
- Zügner, D. and Günnemann, S. Certifiable robustness of graph convolutional networks under structure perturbations. In *SIGKDD*, 2020.
- Zügner, D., Akbarnejad, A., and Günnemann, S. Adversarial attacks on neural networks for graph data. In *SIGKDD*, 2018.

A Details on the experiments and numerical results

Table 3 gives results for node classification. Figure 4 visualizes the number of solved (robust) instances below different time costs, and compares the time costs between SCIPabt and SCIPsbt for MUTAG. Table 4 and Table 5 report the time cost and number of solved instances among all instances and all robust instances for two benchmarks used in graph classification with different budgets. For each benchmark, we present results for ten different global budgets corresponding to 1–10% of edges in the underlying graphs.

Note that we exclude instances with inconsistent results from different solvers, which results in the numbers in column “#” in Table 4 and Table 5 being smaller than the total number of graphs from each benchmark. This is because we found a small bug in Gurobi wherein several instances are declared to be *infeasible* despite having a feasible solution found by SCIP. This bug is easily fixed in Gurobi and will be corrected in its next minor release. So, in fairness to the Gurobi solver, we slightly modified the optimization problems by increasing the right-hand side of Eq. (7c) by 10^{-11} . This change eliminated the bug, but now means that the Gurobi solver frequently returns solutions that are infeasible, i.e., violating some constraints of the MIP model by more than tolerance 10^{-6} . To compare on an equal footing, we only report results on instances where all solvers return consistent answers. In other words, if one solver wrongly declares an instance *infeasible* or returns an infeasible solution, we do not report results.

Table 3: Summary of results for node classification. The approaches tested are SCIP basic (SCIPbasic), SCIP static bounds tightening (SCIPsbt), and SCIP aggressive bounds tightening (SCIPabt). For each global budget, the number of instances is 2708 for Cora and 3312 for CiteSeer. We compare times with respect to both average (“avg-time”) and the shifted geometric mean (“sgm-time”), as well as the number of solved instances within time limits 30 minutes (“# solved”). Since robust instances are the ones where mixed-integer performance is most important (non-robust instances may frequently be found by more heuristic approaches), we also compare on the set of robust instances.

benchmark	method	all instances				robust instances			
		#	avg-time(s)	sgm-time(s)	# solved	#	avg-time(s)	sgm-time(s)	# solved
Cora	SCIPbasic	2708	0.10	0.10	2708	2223	0.08	0.08	2223
	SCIPsbt	2708	0.17	0.16	2708	2223	0.10	0.10	2223
	SCIPabt	2708	0.46	0.38	2708	2223	0.16	0.14	2223
CiteSeer	SCIPbasic	3312	0.07	0.06	3312	2917	0.06	0.06	2917
	SCIPsbt	3312	0.07	0.07	3312	2917	0.06	0.06	2917
	SCIPabt	3312	0.31	0.17	3312	2917	0.12	0.10	2917

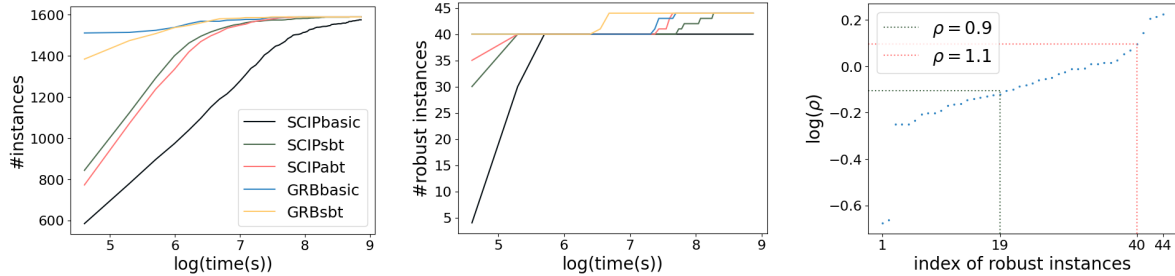


Figure 4: MUTAG benchmark. (left) Number of instances solved by each method below different time costs. (middle) Number of robust instances solved by each method below different time costs. (right) Consider ρ , the ratio of time cost between SCIPabt and SCIPsbt on each robust instance. SCIPabt is at least 10% faster than SCIPsbt on 19 robust instances.

Table 4: Results for ENZYMES with different global budgets. The approaches tested are SCIP basic (SCIPbasic), SCIP static bounds tightening (SCIPsbt), SCIP aggressive bounds tightening (SCIPabt), Gurobi basic (GRBbasic), and Gurobi static bounds tightening (GRBsbt). For each global budget, the number of instances is 600, but we only present comparisons when all methods give consistent results except for time out, as shown in column “#”. We compare times with respect to both average (“avg-time”) and the shifted geometric mean (“sgm-time”), as well as the number of solved instances within time limits 2 hours (“# solved”). Since robust instances are the ones where mixed-integer performance is most important (non-robust instances may frequently be found by more heuristic approaches), we also compare on the set of robust instances.

method	all instances				robust instances			
	#	avg-time	sgm-time	# solved	#	avg-time	sgm-time	# solved
global budget: $[0.01 \cdot E]$								
SCIPbasic	600	465.47	25.13	575	453	420.33	18.76	435
SCIPsbt	600	193.02	14.46	594	453	166.90	10.52	451
SCIPabt	600	190.05	14.58	592	453	161.85	10.53	449
GRBbasic	600	119.88	7.08	594	453	84.71	5.76	451
GRBsbt	600	87.31	5.90	596	453	47.40	4.89	453
global budget: $[0.02 \cdot E]$								
SCIPbasic	597	630.47	37.42	557	392	457.99	18.92	371
SCIPsbt	597	248.67	20.65	585	392	181.41	10.44	385
SCIPabt	597	260.41	21.16	584	392	194.53	10.58	385
GRBbasic	597	170.91	9.36	588	392	111.73	5.05	388
GRBsbt	597	111.66	7.59	592	392	66.45	4.33	391
global budget: $[0.03 \cdot E]$								
SCIPbasic	591	628.77	37.75	556	359	328.18	14.17	347
SCIPsbt	591	252.04	20.87	579	359	117.80	7.67	355
SCIPabt	591	262.35	21.03	577	359	120.84	7.67	354
GRBbasic	591	108.75	8.55	587	359	45.55	3.34	358
GRBsbt	591	79.77	7.05	588	359	22.37	2.79	359
global budget: $[0.04 \cdot E]$								
SCIPbasic	593	633.12	39.29	557	346	256.36	11.96	336
SCIPsbt	593	234.00	21.84	585	346	61.20	6.07	344
SCIPabt	593	253.13	22.90	583	346	62.85	6.13	345
GRBbasic	593	80.87	7.59	591	346	6.44	2.19	346
GRBsbt	593	61.60	6.79	591	346	5.48	1.98	346
global budget: $[0.05 \cdot E]$								
SCIPbasic	591	647.96	41.10	555	338	234.96	10.74	329
SCIPsbt	591	241.04	22.37	581	338	48.19	5.58	337
SCIPabt	591	293.33	23.46	576	338	75.63	5.66	335
GRBbasic	591	72.31	7.61	591	338	6.47	1.99	338
GRBsbt	591	70.81	7.34	589	338	13.86	1.83	338
global budget: $[0.06 \cdot E]$								
SCIPbasic	595	634.72	41.44	560	335	225.61	10.45	327
SCIPsbt	595	219.79	23.28	589	335	54.88	5.49	334
SCIPabt	595	243.19	23.53	586	335	61.32	5.59	333
GRBbasic	595	75.12	7.69	595	335	11.54	2.01	335
GRBsbt	595	65.93	7.20	595	335	37.99	1.93	335
global budget: $[0.07 \cdot E]$								
SCIPbasic	590	635.63	40.99	554	332	195.72	9.84	325
SCIPsbt	590	221.80	23.07	583	332	37.65	5.08	331
SCIPabt	590	259.83	23.68	583	332	54.13	5.25	330
GRBbasic	590	53.62	7.07	590	332	8.03	1.78	332
GRBsbt	590	62.36	7.46	590	332	6.69	1.77	332
global budget: $[0.08 \cdot E]$								
SCIPbasic	583	608.75	39.97	553	332	197.92	9.95	325
SCIPsbt	583	240.35	22.52	575	332	38.82	5.11	331
SCIPabt	583	214.77	22.42	577	332	38.26	5.11	331
GRBbasic	583	60.73	6.92	582	332	8.32	1.85	332
GRBsbt	583	76.61	7.26	582	332	6.03	1.64	332
global budget: $[0.09 \cdot E]$								
SCIPbasic	588	585.39	38.98	557	331	197.91	10.02	324
SCIPsbt	588	241.76	23.02	581	331	43.36	5.08	330
SCIPabt	588	249.56	23.67	580	331	37.99	5.05	330
GRBbasic	588	72.99	7.50	587	331	8.08	1.85	331
GRBsbt	588	75.35	7.23	586	331	6.08	1.66	331
global budget: $[0.10 \cdot E]$								
SCIPbasic	588	602.12	39.14	555	332	205.53	10.01	325
SCIPsbt	588	223.54	22.05	580	332	46.58	5.09	331
SCIPabt	588	237.00	22.88	580	332	41.39	5.07	331
GRBbasic	588	44.81	6.83	588	332	7.72	1.96	332
GRBsbt	588	65.58	7.31	587	332	16.41	1.78	332

Table 5: Results for MUTAG with different global budgets. The approaches tested are SCIP basic (SCIPbasic), SCIP static bounds tightening (SCIPsbt), SCIP aggressive bounds tightening (SCIPabt), Gurobi basic (GRBbasic), and Gurobi static bounds tightening (GRBsbt). For each global budget, the number of instances is 188, but we only present comparisons when all methods give consistent results except for time out, as shown in column “#”. We compare times with respect to both average (“avg-time”) and the shifted geometric mean (“sgm-time”), as well as the number of solved instances within time limits 2 hours (“# solved”). Since robust instances are the ones where mixed-integer performance is most important (non-robust instances may frequently be found by more heuristic approaches), we also compare on the set of robust instances. Note that this test set has no robust instances for global budget $\geq \lceil 0.05 \cdot |E| \rceil$.

method	all instances				robust instances			
	#	avg-time	sgm-time	# solved	#	avg-time	sgm-time	# solved
global budget: $\lceil 0.01 \cdot E \rceil$								
SCIPbasic	124	74.28	45.27	124	24	176.24	162.61	24
SCIPsbt	124	33.89	22.76	124	24	84.37	79.12	24
SCIPabt	124	32.31	22.18	124	24	77.22	72.94	24
GRBbasic	124	2.30	2.16	124	24	4.91	4.82	24
GRBsbt	124	4.10	3.69	124	24	9.39	8.98	24
global budget: $\lceil 0.02 \cdot E \rceil$								
SCIPbasic	141	437.96	87.20	139	16	1028.39	226.02	14
SCIPsbt	141	127.08	37.84	141	16	407.73	115.97	16
SCIPabt	141	98.31	36.72	141	16	287.84	103.45	16
GRBbasic	141	94.67	11.83	141	16	205.18	15.21	16
GRBsbt	141	26.14	8.90	141	16	93.51	17.19	16
global budget: $\lceil 0.03 \cdot E \rceil$								
SCIPbasic	180	542.88	162.56	178	3	4807.52	1181.75	1
SCIPsbt	180	152.61	57.72	180	3	2080.69	545.97	3
SCIPabt	180	134.96	58.51	180	3	1334.79	425.77	3
GRBbasic	180	87.25	10.17	180	3	1245.54	325.46	3
GRBsbt	180	34.48	16.03	180	3	507.82	176.89	3
global budget: $\lceil 0.04 \cdot E \rceil$								
SCIPbasic	174	613.49	199.84	172	1	26.09	26.09	1
SCIPsbt	174	175.59	66.82	174	1	11.45	11.45	1
SCIPabt	174	133.90	67.08	174	1	13.23	13.23	1
GRBbasic	174	49.70	4.59	174	1	1.51	1.51	1
GRBsbt	174	47.76	21.59	174	1	1.55	1.55	1
global budget: $\lceil 0.05 \cdot E \rceil$								
SCIPbasic	167	707.14	233.17	166	—	—	—	—
SCIPsbt	167	185.08	81.61	167	—	—	—	—
SCIPabt	167	170.37	82.49	167	—	—	—	—
GRBbasic	167	23.07	2.30	167	—	—	—	—
GRBsbt	167	61.18	27.22	167	—	—	—	—
global budget: $\lceil 0.06 \cdot E \rceil$								
SCIPbasic	158	832.55	270.16	157	—	—	—	—
SCIPsbt	158	190.53	92.80	158	—	—	—	—
SCIPabt	158	215.46	102.23	158	—	—	—	—
GRBbasic	158	23.74	2.55	158	—	—	—	—
GRBsbt	158	57.60	27.95	158	—	—	—	—
global budget: $\lceil 0.07 \cdot E \rceil$								
SCIPbasic	159	841.40	265.97	158	—	—	—	—
SCIPsbt	159	219.35	94.60	159	—	—	—	—
SCIPabt	159	264.65	112.42	159	—	—	—	—
GRBbasic	159	43.72	2.98	159	—	—	—	—
GRBsbt	159	57.12	25.68	159	—	—	—	—
global budget: $\lceil 0.08 \cdot E \rceil$								
SCIPbasic	159	859.84	265.24	159	—	—	—	—
SCIPsbt	159	254.42	109.18	159	—	—	—	—
SCIPabt	159	299.46	134.91	159	—	—	—	—
GRBbasic	159	4.31	2.18	159	—	—	—	—
GRBsbt	159	65.85	27.45	159	—	—	—	—
global budget: $\lceil 0.09 \cdot E \rceil$								
SCIPbasic	165	877.25	254.34	163	—	—	—	—
SCIPsbt	165	274.26	113.80	165	—	—	—	—
SCIPabt	165	333.40	137.86	165	—	—	—	—
GRBbasic	165	4.26	2.07	165	—	—	—	—
GRBsbt	165	89.31	31.92	165	—	—	—	—
global budget: $\lceil 0.10 \cdot E \rceil$								
SCIPbasic	162	864.13	251.70	159	—	—	—	—
SCIPsbt	162	307.52	120.64	162	—	—	—	—
SCIPabt	162	352.19	149.21	162	—	—	—	—
GRBbasic	162	6.29	2.89	162	—	—	—	—
GRBsbt	162	141.44	49.11	162	—	—	—	—